

**NASA TECHNICAL
MEMORANDUM**

NASA TM X-53661

September 28, 1967

NASA TM X-53661

**LUNAR ENVIRONMENT:
DESIGN CRITERIA MODELS FOR
USE IN LUNAR SURFACE MOBILITY STUDIES**

By Otha H. Vaughan, Jr.
Aero-Astrodynamics Laboratory

NASA

*George C. Marshall
Space Flight Center,
Huntsville, Alabama*

FF No. 602 (C)	N68-10150	(THRU)
	(ACCESSION NUMBER)	1
	47	(CODE)
	(PAGES)	30
	1MX-53661	(CATEGORY)
	(NASA CR OR TMX OR AD NUMBER)	

TECHNICAL MEMORANDUM X-53661

LUNAR ENVIRONMENT: DESIGN CRITERIA MODELS FOR USE
IN LUNAR SURFACE MOBILITY STUDIES

By

Otha H. Vaughan, Jr.

George C. Marshall Space Flight Center

Huntsville, Alabama

ABSTRACT

The photographic data obtained by the Ranger (VII, VIII and IX), the Surveyor I, the Orbiter I, II and III, and Russia's Luna IX and XIII space vehicles have been analyzed and interpreted in the development of lunar terrain models for use in the design of lunar roving vehicles. An attempt has been made to make the design criteria as realistic as possible with the information now available from these lunar probes. As additional information about the lunar surface is gained from additional flights of the Surveyor series, these models will be re-evaluated and revised whenever necessary.

NASA - GEORGE C. MARSHALL SPACE FLIGHT CENTER

NASA - GEORGE C. MARSHALL SPACE FLIGHT CENTER

Technical Memorandum X-53661

September 28, 1967

LUNAR ENVIRONMENT: DESIGN CRITERIA MODELS FOR USE
IN LUNAR SURFACE MOBILITY STUDIES

By

Otha H. Vaughan, Jr.

AEROSPACE ENVIRONMENT DIVISION
AERO-ASTRODYNAMICS LABORATORY
RESEARCH AND DEVELOPMENT OPERATIONS

TECHNICAL MEMORANDUM X-53661

LUNAR ENVIRONMENT: DESIGN CRITERIA MODELS FOR USE IN LUNAR SURFACE MOBILITY STUDIES

SUMMARY

A series of baseline models has been developed for use in the design of lunar roving vehicles for manned lunar exploration. The mobility capability requirements of a lunar roving vehicle must be established at the present time on data obtained from the interpretation of the photographic data of Ranger, Surveyor, and Orbiter, and the Russian Luna IX and XIII probes. The models presented in this report are based on the author's interpretation of these photographic data, on a review of the literature, and on extensive discussions with representatives of such agencies as JPL, USGS Branch of Astrogeology, and the Lunar and Planetary Laboratory of the University of Arizona. The literature survey, as well as the personal discussions, revealed that personnel of the scientific community who are primarily concerned with interpretation of the data obtained by the cameras of the various lunar probes are not in complete agreement among themselves so, of course, complete agreement with the interpretations presented herein cannot be anticipated. One of the difficulties stems from the fact that the photographs from the various probes are of different areas of mare surface so that real geophysical differences and differences in interpretation are intermingled. Since the best available data have been obtained from this lunar photography, a great deal of reliance at the present time has been placed on these data for purposes of establishing design criteria for lunar roving vehicles.

I. INTRODUCTION

The Ranger, Orbiter, and the Surveyor programs were established for the purpose of obtaining the most information possible about the surface and environment of the moon for use in determining the requirements for eventually landing a man on the moon, for his survival in this unique environment, and for exploration of the lunar surface. Although these lunar probes have yielded a wealth of photographic information about the lunar environment, there is much disagreement among scientists regarding the interpretation of such data, especially in determining the bearing strength and cohesiveness of soil and whether the surface features are due to volcanic activity or meteoroid impact. These factors have great significance not only for safely landing a man on the moon, but also for

his mobility while on the surface, and for his safe return to earth. The various data have been interpreted in this report specifically for the development of lunar terrain models on which to base design criteria for lunar roving vehicles.

The mare areas on the moon, such as Oceanus Procellanum where the Surveyor I landed at 06:17:37 GMT on June 2, 1966, were believed to be the smoothest and most suitable for a landing site for manned spacecraft. The mare terrain models in this report, therefore, are based on photographic information of this area, and other mare areas, from the Orbiter series (for crater count) and from the Surveyor I spacecraft (for boulder count, surface roughness, and soil texture).

Current lunar exploration vehicles were designed on the basis of less accurate information than is now available as a result of the various programs referenced above. The author believes that the dark, regional, smooth-rayed, and rough-rayed mare models presented herein are the most realistic possible based on the data now available. While these models were being developed, the Surveyor III successfully soft-landed on the moon on April 20, 1967. Before the report was completed, Surveyor V made a successful soft-landing on September 10, 1967. Data from both of these spacecraft, when they have been analyzed and become available, should result in even more realistic models that are applicable to broader areas of the maria. Also, photographs of higher resolution from Orbiter IV and V spacecraft will become available. Thus, the "guesses" and estimates will be gradually removed, more realistic lunar surface models will be defined, and better lunar vehicles can be designed.

A. Composition of the Mare Surface

1. Luna IX and XIII Data

Russia's Luna IX spacecraft, after surviving the impact of landing, provided a wealth of photographic information about the mare areas of the lunar surface, especially the bearing strength and cohesion of the soil. The fact that the spacecraft did not sink in the soil to any appreciable depth implies that the mare surface does indeed have a finite bearing strength, estimated by Scott in his analysis [1] at about 2 to 4 psi. Luna IX, which landed in Oceanus Procellarum, produced the first photographs of small-scale lunar structures. One photograph (figure 1) showed many boulders ranging in size from three meters to smaller than 10 cm and many craters some as large as 17 meters in diameter, the smaller ones producing an undulating appearance of the terrain. The Luna IX cameras also photographed numerous small rocks that, even though they had landed at some velocity, seemed not to have

penetrated the soil to any great depth. The mare soil appeared vesiculated, or composed of a rubble of fine-grained material. The question still remains, however, as to whether the soil at the Luna IX landing site is of volcanic activity or meteorite impact origin. It could have been created by volcanic action because of its similarity, as seen in the photography, to scoriaceous lava of the AA type. On the other hand, the fine-grained material could be the result of meteoroid impact because of its similarity to ejecta from meteoroids striking the earth and to ejecta from underground nuclear explosions.

Luna IX also provided some indication of the cohesiveness of the mare soil. This information was obtained in a study by the author [2] of stereoscopic images of the small craters at the Luna IX landing site. Some of these craters appear to have raised rims; if this analysis is correct, the soil around the rims of the craters is cohesive to some extent, based on studies of terrestrial craters by Gault and Quaide [3] and Moore and Shoemaker [4].

Luna XIII [5] data indicated that the mare surface at the landing site was not hard rock as supposed by some, but the upper layers (7.7 to 27.9 cm) of the surface had a density of approximately 1 gram/cc. The Luna XIII photographs provided additional information on the size and distribution of craters and rock-like objects already seen in the Luna IX photographs. Figure 2, a plot of the distribution of boulders as seen in the Luna IX photography, was produced by Smith in reference 14.

The cameras on the Luna IX and Luna XIII spacecraft did not produce enough information to establish whether the surface features they photographed were of volcanic origin or whether they were produced by meteoroid impact. However, Luna IX gave us the first look at the surface of the moon at close range, and helped to establish the fact that, insofar as the surface bearing strength and cohesiveness was concerned, man and his equipment could land and operate on the lunar surface for some period of time.

2. Surveyor I and Orbiters I, II and III Data

Surveyor I soft-landed on the floor of Oceanus Procellarum on June 2, 1966, about 5 months after the Luna IX had landed. The photographs from the Surveyor I were of higher resolution and thus gave a better indication of the actual texture of the soil at its landing site. As a matter of fact, it was definitely established that the soil at the Surveyor I site is composed of a mixture of fine-grained particles (figure 3) and is littered in some areas with boulders and ejecta (figures 4 and 5). Also, the terrain as seen by the Surveyor I cameras is pockmarked with numerous craters ranging in size from a few centimeters

to 80 meters in diameter. The smaller craters (see figure 6), ranging from a few centimeters to 3 meters in diameter, cover about 50 percent of the surface [7]. The rims of the larger craters (see figure 7), with diameters ranging in size from 80 meters down to about 6 meters, were strewn with blocky material, indicating that the thickness of the fragmental layer of fine material extends from about one meter to approximately 15 meters above the bed-rock, which is mantled by this fragmental layer. The angular shape of the ejected rock indicates that the bed-rock material is relatively strong.

Orbiter II photographs (see figure 8a) have also shown a large amount of blocky material lying in and near the large craters. Some of the largest craters, ranging from about 60 to 200 meters in diameter, look strikingly similar to Danny Boy (figure 8b), a man-made terrestrial crater created by an underground nuclear explosion. Trafficability near fresh craters of these types will probably be limited within approximately two crater diameters, since some of the blocky debris which can be resolved are much larger than one meter even at two crater diameters distance from the source of the primary crater producing the ejecta. Cumulative size versus frequency distribution of craters and particles on the surface near the Surveyor site is shown in figures 9a and 9b. A cumulative size versus frequency distribution of craters (30 to 400 meters) based on Orbiter I data near the approximate area of the Surveyor I site is shown in figure 10. In addition to the blocky-type craters, there are certain craters seen in Orbiter II data which have a patterned-ground appearance. These craters appear to be filling because of the slumping of materials toward the floor of the crater (figure 11). Other areas of the lunar surface, as seen from Orbiter II data (figure 12), appear to be smoother than might be expected, because of the presence of possible volcanic materials which appear to have subdued the craters and their blocky type ejecta roughness resulting from impacts. Orbiter III data also showed large amounts of blocky ejecta, confirming that the lunar surface has quite a spectrum of roughness. Thus, at the present time, one can only estimate what a possible realistic model of the lunar surface might be like based on the very small "ground truth" data samples and photography.

B. Discussion of Baseline Terrain Models

The design of roving or flying vehicles for exploring the lunar surface requires a knowledge of the lunar terrain and its characteristics. Most important to the designer are those parameters which describe the surface in terms of roughness, slope distributions, soil characteristics, and the various obstacles which may be encountered by this vehicle during its normal operation.

To provide a vehicle designer with data which will describe as many of the types of conditions or obstacles which may be encountered, baseline terrains for use as design criteria were developed. Since the vehicles will be required to operate over a series of terrains, different in terms of their roughness and various types of soil characteristics, the models, as presented, depict a spectrum of increasing roughness. These terrain models are classified as: Dark Regional Mare, the Smooth Regional Mare, the Smoothed-Rayed Mare, and the Rough-Rayed Mare. A model for each of these types of terrain will be discussed in the following sections.

II. BASELINE TERRAIN MODELS AND SUPPORTING INFORMATION

1. The Dark Mare Model

Before the landing of the Surveyor I spacecraft, those areas on the moon which were dark in texture (low albedo, 0.068, based on earth-based telescope observations) were considered to be the smoothest areas and thus the most suitable for the landing of a spacecraft. These areas have very low median slopes (1°) based on a 1 km interval for the slope measurement, as expressed by McCauley [8] in his terrain analysis (see figures 13a and b). Interpretation of data generated from Ranger 7 by McCauley and Rowan [9] indicated that the median slope based on a one-meter resolution for the dark mare at the Ranger 7 impact area was approximately 7° (figure 14). Thus, the Ranger 7 provided another sample of information on surface roughness at the one-meter resolution. However, the fact that there were no one-meter or larger blocks in the mare area photographed by Ranger 7 was very misleading, since this seemed to imply that most of these types of mare terrain were free of blocky material. Ranger 8, however, indicated that there was some blocky material lying on the surface of the mare particularly near large craters (figure 15). In addition, Surveyor I and Luna IX and XIII established that the mare areas in some locations do have variable amounts of blocky material one meter or less around craters whose diameters are even as small as three meters. Thus, these data imply that the fragmental layer, particularly at the Surveyor I site, is relatively thin (one meter to two meters), but possibly quite variable in thickness at other places in this and other areas. Recent Orbiter III photos (figure 16) of the Surveyor I site have helped to provide some measure of the thickness of this fragmental layer by a study of the similarity of the various small diameter craters and their blocky ejecta distribution along with the data from controlled cratering experiments performed on the earth. Thus, the dark-mare model has been developed on the basis of interpretation of the Surveyor I data supported by Orbiter data. The general terrain in the area of the Surveyor I site close to the spacecraft appears to be relatively flat with many small rock-like obstacles and

craters (figures 4, 5, 6, and 7). Thus, any vehicle operating on this type of terrain must be able to negotiate (climb or straddle) small obstacles of 20 to 30 cm or less and be able to steer around an occasional one-meter or larger block every 100 m² of the surface area. This terrain appears to be pockmarked by craters with diameters in the range of a few centimeters to five meters and above. This type of roughness will require a certain amount of reserve power for climbing in and out of these smaller craters (two meters or less) which cannot be avoided. A typical slope distribution considered by the author to be representative of this terrain is shown in table I.

The following crater distributions are considered to be representative of the minimum number of craters which may be expected to occur in this particular baseline terrain in the vicinity of a certified LM landing site (50 km² area):

- (1) 10,000 craters, 1 to 10 meters in diameter,
- (2) 6,500 craters, 10 to 20 meters in diameter,
- (3) 1,200 craters, 20 to 30 meters in diameter,
- (4) 400 craters, 30 to 40 meters in diameter,
- (5) 500 craters, 40 meters or larger in diameter.

The craters are considered to be randomly distributed and the craters in the 20- to 30-meter range are considered to have blocky ejecta (1 meter or less) within a radius of 2 crater diameters from the center of the primary.

Although the mobility power requirements can be computed for steady state operation (no dynamics) based on the slope distribution for a baseline terrain, data are still required to describe the surface roughness of the terrain which may be superimposed on the normal slope trend and at a scale which directly affects vehicle dynamics.

In general, vehicles in off-the-road operations on the earth or on the lunar or planetary surface will encounter at least two types of "hard ground" roughness. Obstacles such as large craters, large boulders, cracks, and abrupt collapses of the topography are considered as one type of ground roughness. Trafficability by the vehicle in this type of ground roughness depends on the driver and the vehicle obstacle capabilities and geometry; i.e., what is an obstacle to one vehicle is not an obstacle to another. The other type of roughness consists of

variations in elevations which are stable over reasonably large areas (small craters, crevices, and small rocks) but change gradually with distance is called "stable-ground roughness." Rapid traversability over this type of roughness is a function of vehicle geometry, suspension systems, speed, types of cargo, and driver comfort. Designers of off-the-road vehicles have turned to the use of statistical techniques or power spectral density estimates (P.S.D.) to characterize stable-ground roughness for predicting vehicle performance and improving the performance characteristics (vehicle speed, comfort, controllability, etc.). No information has yet been developed on the power spectral density for the Surveyor I landing site.

However, preliminary power spectral estimates of the roughness content of a sample of lunar mare by Jaeger [10] and Van Deusen [11] have been developed based on an analysis of topographic data generated from the small areas photographed in high resolution during the Ranger VII and VIII missions. Van Deusen [11] in his study concluded that the P.S.D. of natural terrains can be expressed in the following form:

$$P(\Omega) = K\Omega^N$$

where $P(\Omega)$ is the P.S.D. of the surface displacement (profile height) in units of meters²/cycles/meter, Ω is the spatial frequency in cycles/meter, and K and N are constants for any given spectral estimates. In addition, Van Deusen [11] concluded that natural surfaces have not favored a predominant frequency and that the value of N is approximately -2. Thus, for the purposes of this report, the author, using the data generated by Jaeger and Van Deusen as well as his own subjective analysis of the Orbiter data, has concluded that the lunar mare terrain in some locations will be somewhat smoother than indicated by the Surveyor I and is in some locations considerably rougher than a spectrum of roughness that the author has seen on the earth (e.g., old volcanoes and those craters caused by nuclear explosions). Thus, the P.S.D. information presented in this report reflect the author's "most realistic" interpretation of the expected "stable-ground" roughness in the various types of mare terrains. Although these P.S.D. estimates cannot yet be verified by actual topographic data, analysis of Surveyor and Orbiter data can, hopefully, provide this type of data at a later time. Therefore, it is believed that the following P.S.D. function is more representative of the "stable-ground" roughness of the dark regional mare terrain.

$$P(\Omega) = K\Omega^N$$

where

$$K = 2.4 \times 10^{-4}$$

Ω = frequency range 0.05 to 0.5 cycles/meter

$$N = -2.$$

2. The Regional Mare Model

The regional-type mares are those areas on the lunar surface which have albedos generally in the range from 0.075 to 0.090 and are characterized by moderate slopes and pronounced heterogeneity. Superimposed on the basic mare material are ridges, crater fields, irregular depressions, subdued craters, domes, rilles, etc., which help to contribute to the roughness of this type of terrain. A terrain model is best developed by using an analysis of the photographic data from Orbiters I and II. The slope distributions presented in table II are considered as representative of this type of terrain while a photograph of the typical terrain sample for this type mare is shown in figure 17. Since there has been no landing in this particular type of terrain to show the small-scale roughness which affects vehicle mobility, an index of roughness must be estimated at the present time. Therefore, the following power spectral density function is recommended as a statistical model for this type of terrain:

$$P(\Omega) = K\Omega^N \quad \text{m}^2/\text{cycles/m}$$

where

$$K = 4.3 \times 10^{-4}$$

Ω = 0.05 to 0.5 cycles/m

$$N = -2.$$

The following crater distributions are considered to be representative of the minimum number of craters which can be expected to occur in this particular baseline terrain in the vicinity of a certified LM landing site (50 km² area):

- (1) 15,000 craters 1 to 10 meters in diameter,
- (2) 11,600 craters 10 to 20 meters in diameter,
- (3) 1,620 craters 20 to 30 meters in diameter,

- (4) 200 craters 30 to 40 meters in diameter,
- (5) 440 craters 40 meters or larger in diameter.

The craters are considered to be randomly distributed and the craters in the 20- to 30-meter range are considered to have blocky ejecta (1 meter or less) within a radius of 2 crater diameters from the center of the primary:

3. The Smooth-Rayed Mare Model

The smoothed-rayed areas in the mare are those areas of the dark regional mare upon which a mixture of blocky rubble (large and small sizes) and fine-grained materials have been deposited. These areas have albedo in the range from 0.088 to 0.096 and many of the smaller craters and their ejecta have been somewhat subdued by the presence of a fine-grained material produced either by volcanos or meteoroid impact. Certain areas of this terrain will be littered by one-meter or larger boulders ejected from the surface by the impact of bodies with energy sufficient to penetrate into the harder materials below the fragmental layer. The terrain in some areas will be smoother than the dark regional mare area (as seen by Surveyor I) in terms of crater distribution. A typical slope distribution considered to be representative of this terrain is shown in table III. A photograph of the typical terrain sample for this type of mare is shown in figure 18. The following crater distributions are considered to be representative of the minimum number of craters which can be expected to occur in this particular baseline terrain in the vicinity of a certified LM landing site (50 km² area):

- (1) 12,000 craters 1 to 10 meters in diameter,
- (2) 8,800 craters 10 to 20 meters in diameter,
- (3) 300 craters 20 to 30 meters in diameter,
- (4) 140 craters 30 to 40 meters in diameter,
- (5) 400 craters 40 meters or larger in diameter.

The craters are considered to be randomly distributed and the craters in the 20- to 30-meter range are considered to have blocky ejecta (1 meter or less) within a radius of 2 crater diameters from the center of the primary.

Since there has been no landing in this particular type of terrain to show the small-scale roughness which affects vehicle mobility, an index of roughness must be estimated at the present time. Therefore, the following power spectral density function is recommended as a statistical model for this type of terrain:

$$P(\Omega) = K\Omega^N \quad \text{m}^2/\text{cycles/m}$$

where

$$K = 3.6 \times 10^{-4}$$

$$\Omega = 0.05 \text{ to } 0.5 \text{ cycles/meter}$$

$$N = -2.$$

4. The Rough-Rayed Mare Model

The rough-rayed areas in the mare are those areas of the regional mare upon which a large amount of the ejecta from the fresh-impact crater has not been subdued by a deposition of fine-grained materials. The rough-rayed areas are those which have albedos in the range of 0.096 to 0.114. The main roughness in these areas will be the result of the many slope reversals due to the presence of secondary craters which have not been filled by fine-grained materials. Roughness will also be due to the rough ejecta blankets (boulder fields) produced by those bright craters which have penetrated into the bedrock, thus ejecting blocky type materials. A typical slope distribution is shown in table IV. A photograph of the typical terrain sample for this type of mare is shown in figure 19. The following crater distributions are considered to be representative of the minimum number of craters which can be expected to occur in this particular baseline terrain in the vicinity of a certified LM landing site (50 km² area):

- (1) 20,000 craters 1 to 10 meters in diameter,
- (2) 14,500 craters 10 to 20 meters in diameter,
- (3) 500 craters 20 to 30 meters in diameter,
- (4) 130 craters 30 to 40 meters in diameter
- (5) 500 craters 40 meters or larger in diameter.

The craters are considered to be randomly distributed, and the craters in the 20- to 30-meter range are considered to have blocky ejecta (1 meter or less) within a radius of 2 crater diameters from the center of the primary.

Since there has been no landing in this type of terrain, to show the small scale roughness which affects mobility, an index of roughness of this type terrain must be estimated at the present time. Therefore, the following power spectral density function is recommended as the statistical model for this type of terrain:

$$P(\Omega) = K\Omega^N \quad \text{m}^2/\text{cycles/m}$$

where

$$K = 5.8 \times 10^{-4}$$

$$\Omega = 0.05 \text{ to } 0.5 \text{ cycles/meter}$$

$$N = -2.$$

5. Coefficient of Friction of Lunar Surface Materials

The actual coefficient of friction data for metallic materials in contact with the lunar surface materials has not been established at the present time. Recent laboratory data by Fields [13] have indicated that the coefficient of friction between both basalt powders (250 to 500 microns in diameter) and aluminum plates was 0.21 under atmospheric pressure, increasing to .28 under a pressure of 10^{-7} torr. Fields noticed that, as the vacuum increases, the coefficient of friction increases. Thus, at the present time, the recommended value for the average coefficient of friction for this report is 0.6. This value is to be used when performing obstacle-climbing and crevice-crossing calculations when determining specific vehicle mobility characteristics. Minimum values for the coefficient of internal friction for lunar soil materials at the surface to a depth of a few centimeters is estimated to be 0.46 [12]; however, for draw-bar-pull calculations, the proposed value to be used with each of the terrain soil models in this report is 0.4 to 0.7.

III. CONCLUDING REMARKS

A series of lunar surface models has been developed for use in an attempt to provide realistic design criteria for roving vehicles. Since a lunar exploration vehicle will be required to land and/or traverse through areas which are of interest to the geologist, it appears that the most interesting areas will probably also be the roughest. Therefore, the proposed models cover the possibility that a vehicle which is designed today on best available data can still be useful if it is later required to operate in somewhat rougher terrains than those which can be seen in the 1-meter resolution (Orbiter) photographs. As better terrain, soil, and roughness information become available, the proposed models will be updated to reflect the increased knowledge, and thus the vehicle systems can be optimized.

TABLE I

Dark Regional Mare

<u>Slope Angle*</u> <u>(degrees)</u>	<u>Percent of Total***</u> <u>Distance</u>	<u>Soil Constants**</u>
2	56.0	$K_{\phi} = 0.5$ $N = 0.5$
4	20.0	Very fine grained material.
6	15.0	
10	4.7	$K_{\phi} = 1.0$ $N = 0.75$ Medium grained fragmental material
20	3.8	$K_{\phi} = 3.0$ $N = 1.0$ Loose type fragmental material.
30	0.3	$K_{\phi} = 6.0$ $N = 1.25$ A bonded fragmental material similar to hard sand.
35	0.2	$K_{\phi} = 6.0$ $N = 1.25$

* The distribution of slopes for this terrain is 50/50; i.e., +2° slopes cover 28 percent of total distance.

** Soil is assumed to be cohesionless frictional type soil ($c = 0$, $K_c = 0$) at the present time even though the Surveyor I landing data implies a very small amount of cohesion is present in the lunar soil. The slippage coefficients are $K_1 = 0.2$ and $K_2 = 1.25$.

*** The slope distributions are based on a series of typical scientific mission traverses from a landing site and the distribution represents a total travel distance of 100 kilometers.

TABLE II

Regional Mare

<u>Slope Angle*</u> <u>(degrees)</u>	<u>Percent of Total***</u> <u>Distance</u>	<u>Soil Constants**</u>
2	16.0	$K_{\phi} = 0.5$ $N = 0.5$
4	35.0	Very fine grained material.
6	20.0	
10	15.0	$K_{\phi} = 1.0$ $N = 0.75$ Medium grained fragmental material.
20	8.3	$K_{\phi} = 3.0$ $N = 1.0$ Loose type fragmental material.
30	5.1	$K_{\phi} = 6.0$ $N = 1.25$ A bonded fragmental material similar to hard sand.
35	0.6	$K_{\phi} = 6.0$ $N = 1.25$

* The slope distribution of slopes for this terrain is 50/50; i.e., +2 slopes cover 8 percent of total distance.

** Soil is assumed to be cohesionless frictional type soil ($c = 0$, $K_c = 0$) at the present time even though the Surveyor I landing data implies a very small amount of cohesion is present in the lunar soil. The slippage coefficients are $K_1 = 0.2$ and $K_2 = 1.25$.

*** The slope distributions are based on a series of typical scientific mission traverses from a landing site and the distribution represents a total travel distance of 100 kilometers.

TABLE III

Smooth-Rayed Mare

<u>Slope Angle*</u> <u>(degrees)</u>	<u>Percent of Total***</u> <u>Distance</u>	<u>Soil Constants**</u>
2	44.7	$K_{\phi} = 0.5$ $N = 0.5$
4	24.0	Very fine grained material.
6	15.7	
10	5.3	$K_{\phi} = 1.0$ $N = 0.75$ Medium grained fragmental material.
20	8.0	$K_{\phi} = 3.0$ $N = 1.0$ Loose type fragmental material.
30	2.2	$K_{\phi} = 6.0$ $N = 1.25$ A bonded fragmental material similar to hard sand.
35	0.1	$K_{\phi} = 6.0$ $N = 1.25$

* The distribution of slopes for this terrain is 50/50; i.e., +4° slopes cover 12 percent of total distance.

** Soil is assumed to be cohesionless frictional type soil ($c = 0$, $K_c = 0$) at the present time even though the Surveyor I landing data implies a very small amount of cohesion is present in the lunar soil. The slippage coefficients are $K_1 = 0.2$ and $K_2 = 1.25$.

*** The slope distributions are based on a series of typical scientific mission traverses from a landing site and the distribution represents a total travel distance of 100 kilometers.

TABLE IV
Rough-Rayed Mare

<u>Slope Angle*</u> (degrees)	<u>Percent of Total***</u> <u>Distance</u>	<u>Soil Constants**</u>
2	8.0	$K_{\phi} = 0.5$ $N = 0.5$
4	16.0	Very fine grained material.
6	23.0	
10	25.0	$K_{\phi} = 1.0$ $N = 0.75$ Medium grained fragmental material
20	16.0	$K_{\phi} = 3.0$ $N = 1.0$ Loose type fragmental material
30	8.2	$K_{\phi} = 6.0$ $N = 1.25$ A bonded fragmental material similar to hard sand.
35	3.8	$K_{\phi} = 6.0$ $N = 1.25$

* The distribution of slopes for this terrain is 50/50; i.e., +4° slopes cover 8 percent of total distance.

** Soil is assumed to be cohesionless frictional type soil ($c = 0$, $K_c = 0$) at the present time even though the Surveyor I landing data implies a very small amount of cohesion is present in the lunar soil. The slippage coefficients are $K_1 = 0.2$ and $K_2 = 1.25$.

*** The slope distributions are based on a series of typical scientific mission traverses from a landing site and the distribution represents a total travel distance of 100 kilometers.



Figure 1. Luna IX Panorama of Lunar Surface Taken Early Feb. 4, 1966
(Large Rock Close to Spacecraft, 15 cm Diameter)

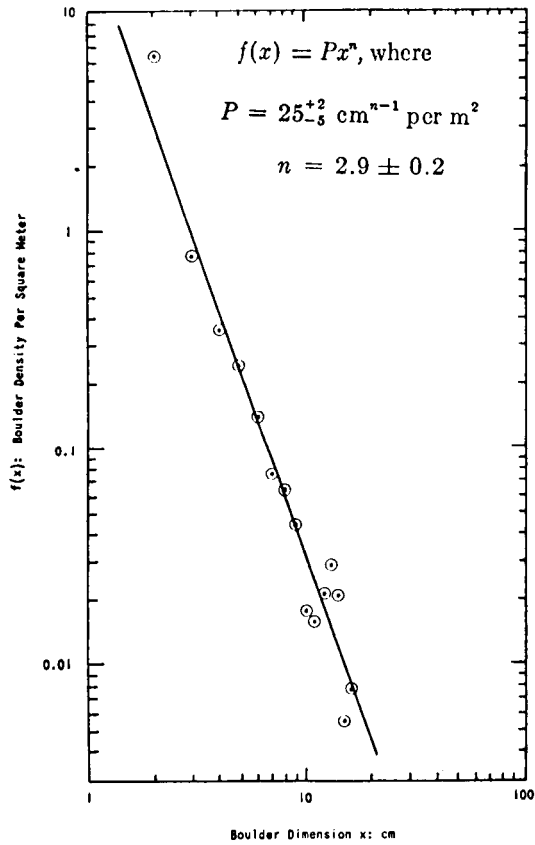


Figure 2. Surface Distribution of Boulders (Smith)

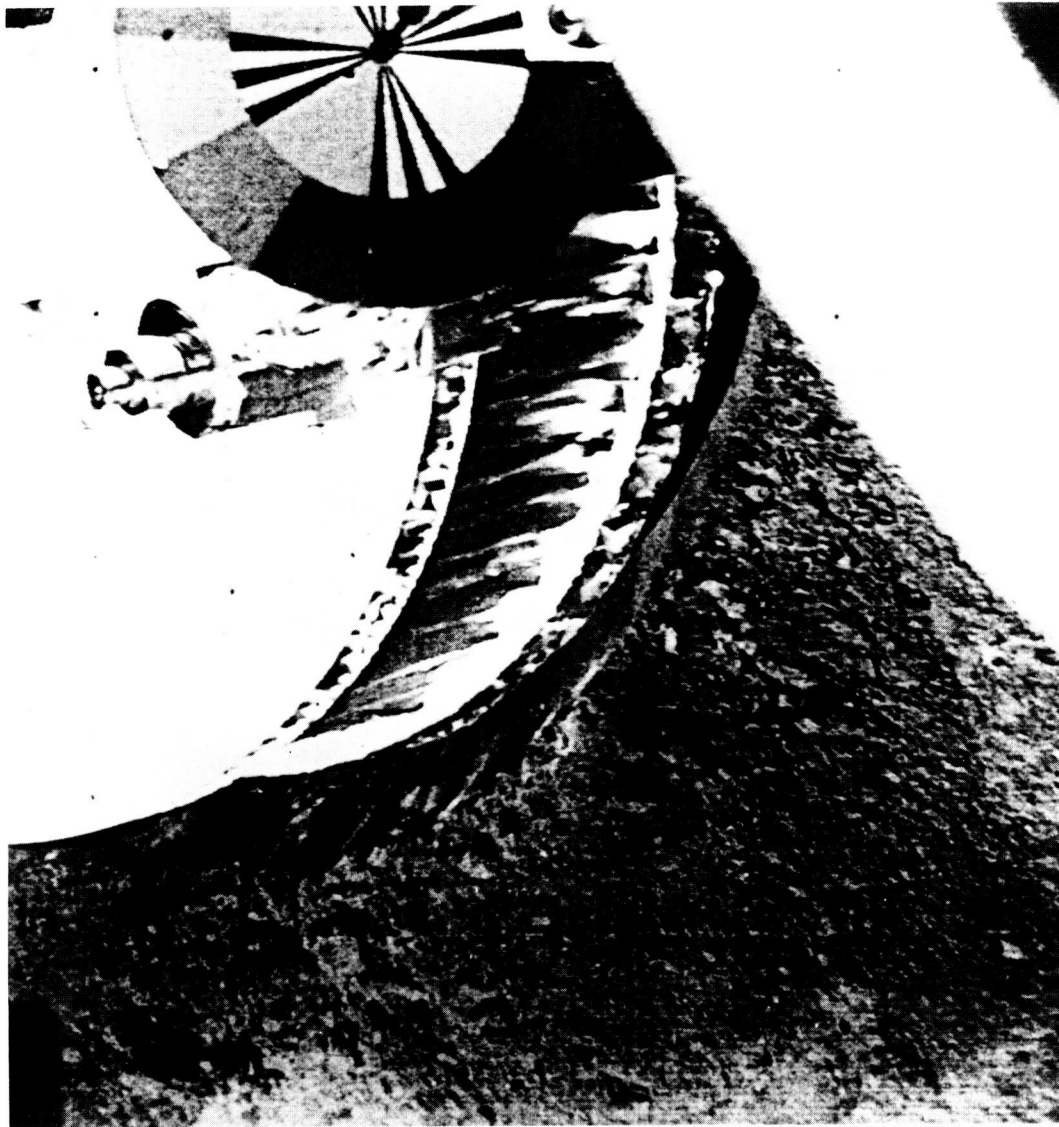


Figure 3. Fine Grained Soil at Surveyor I Landing Site
(Smallest particles .5 mm can be resolved)

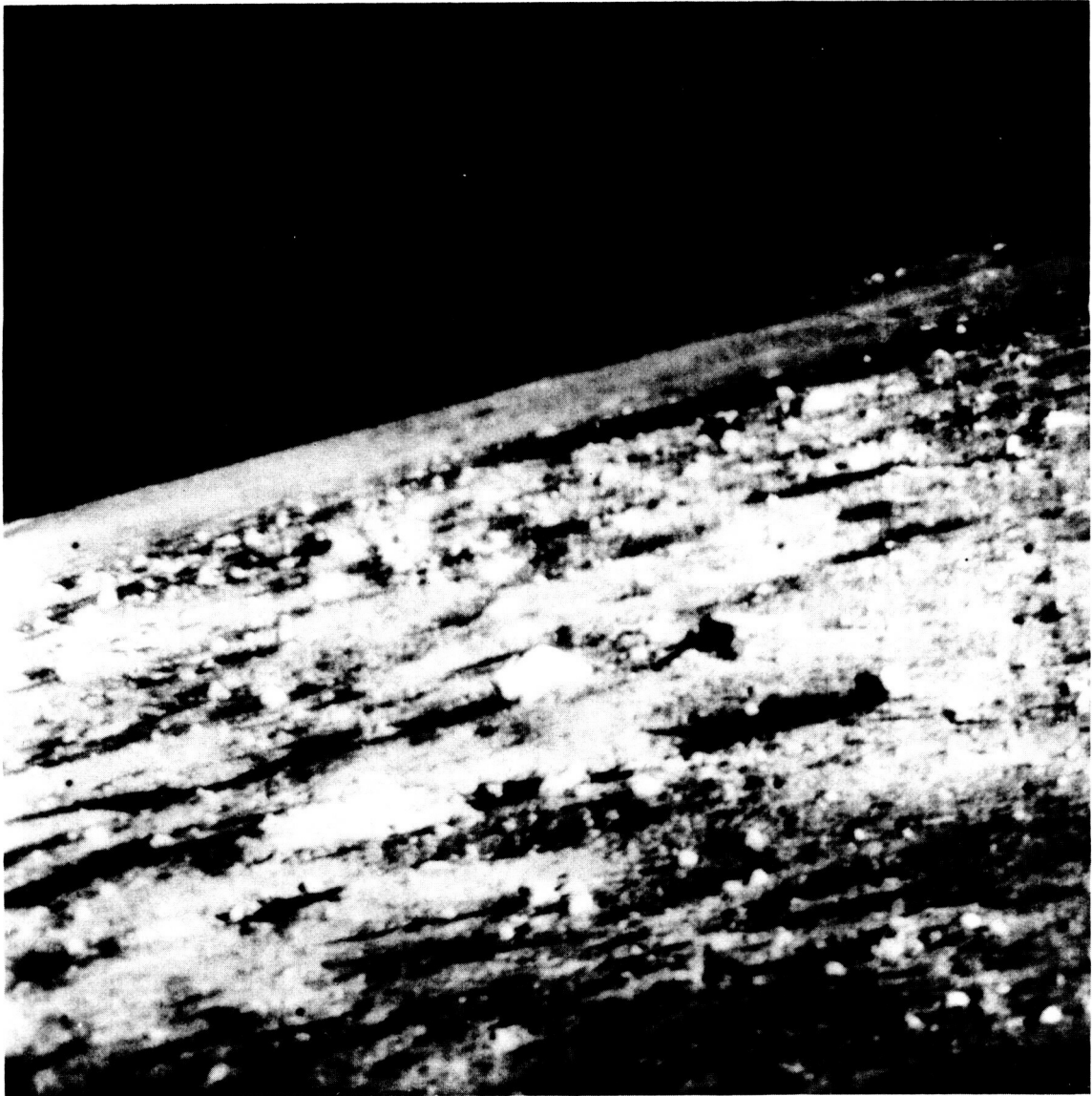


Figure 4. Boulders and Small Ejecta-Type Strewn Terrain
Near Surveyor I Landing Site
(20 cm to 1 meter boulders)



Figure 5. Mosaic of Surveyor I Site Looking Eastward (Lunar Afternoon)

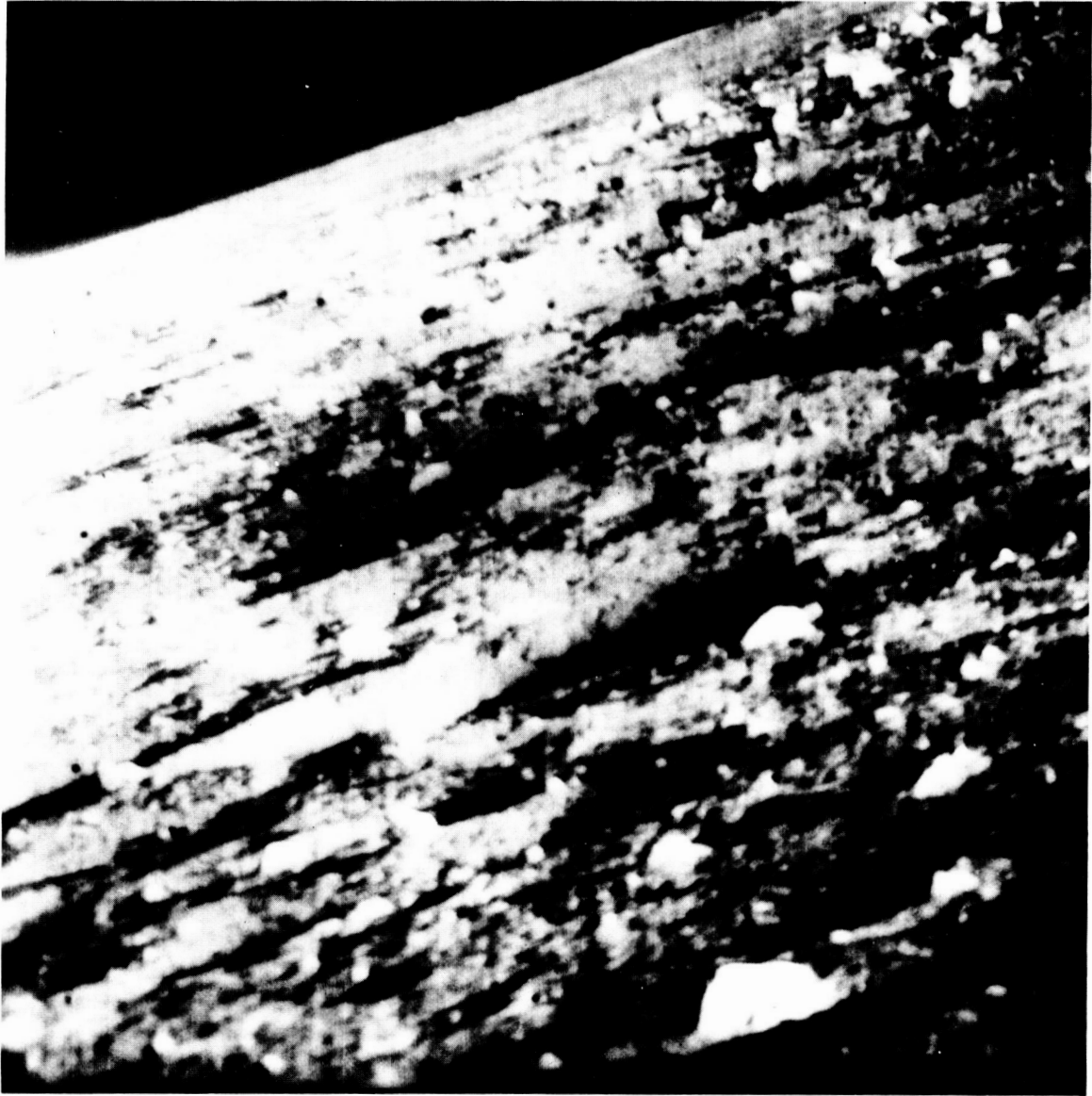


Figure 6. Small Craters (1 cm to 3 m Size Range)

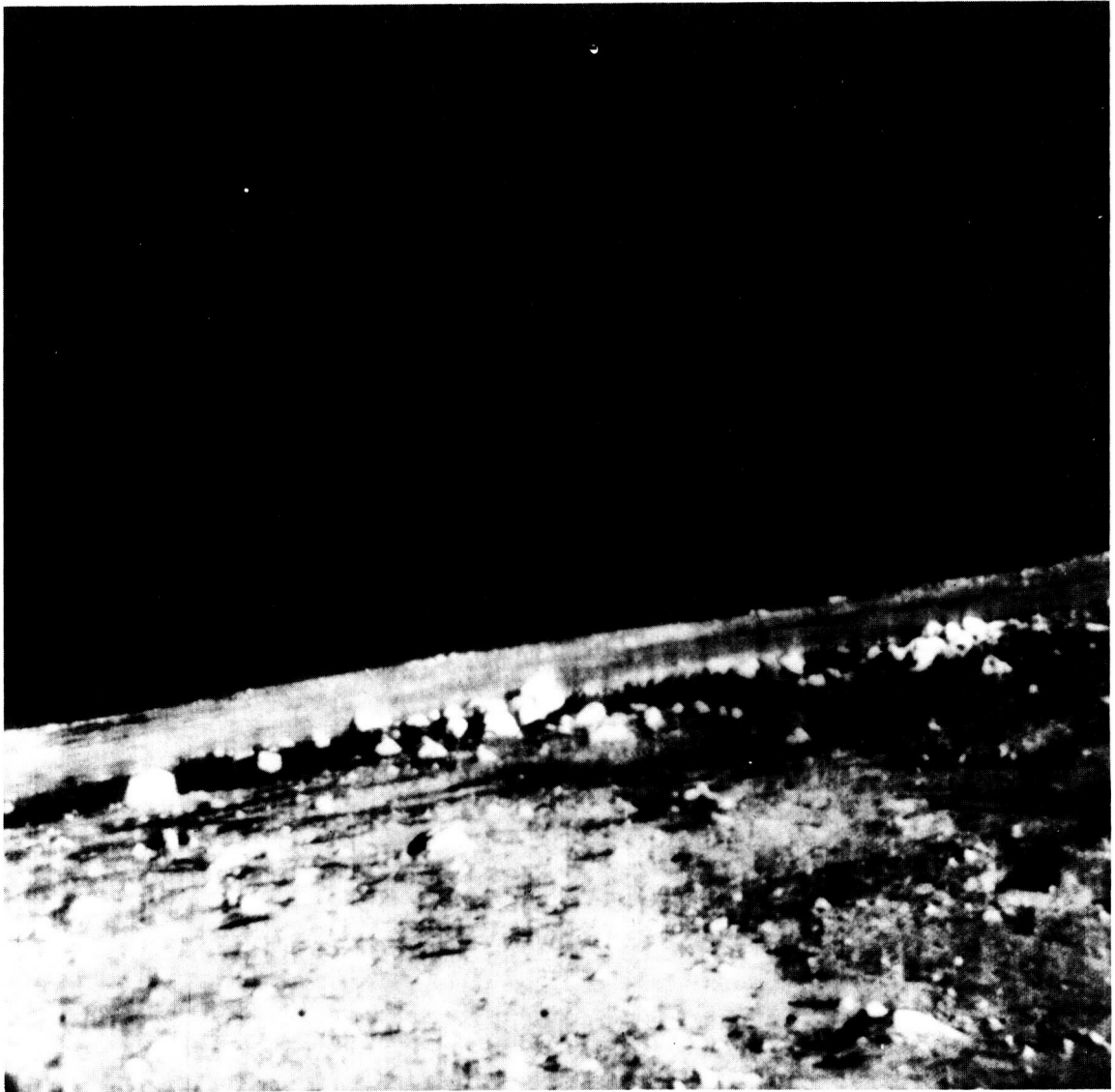


Figure 7. Large Crater and Blocky Ejecta Materials
(20 cm to 3 meter diameter ejecta)

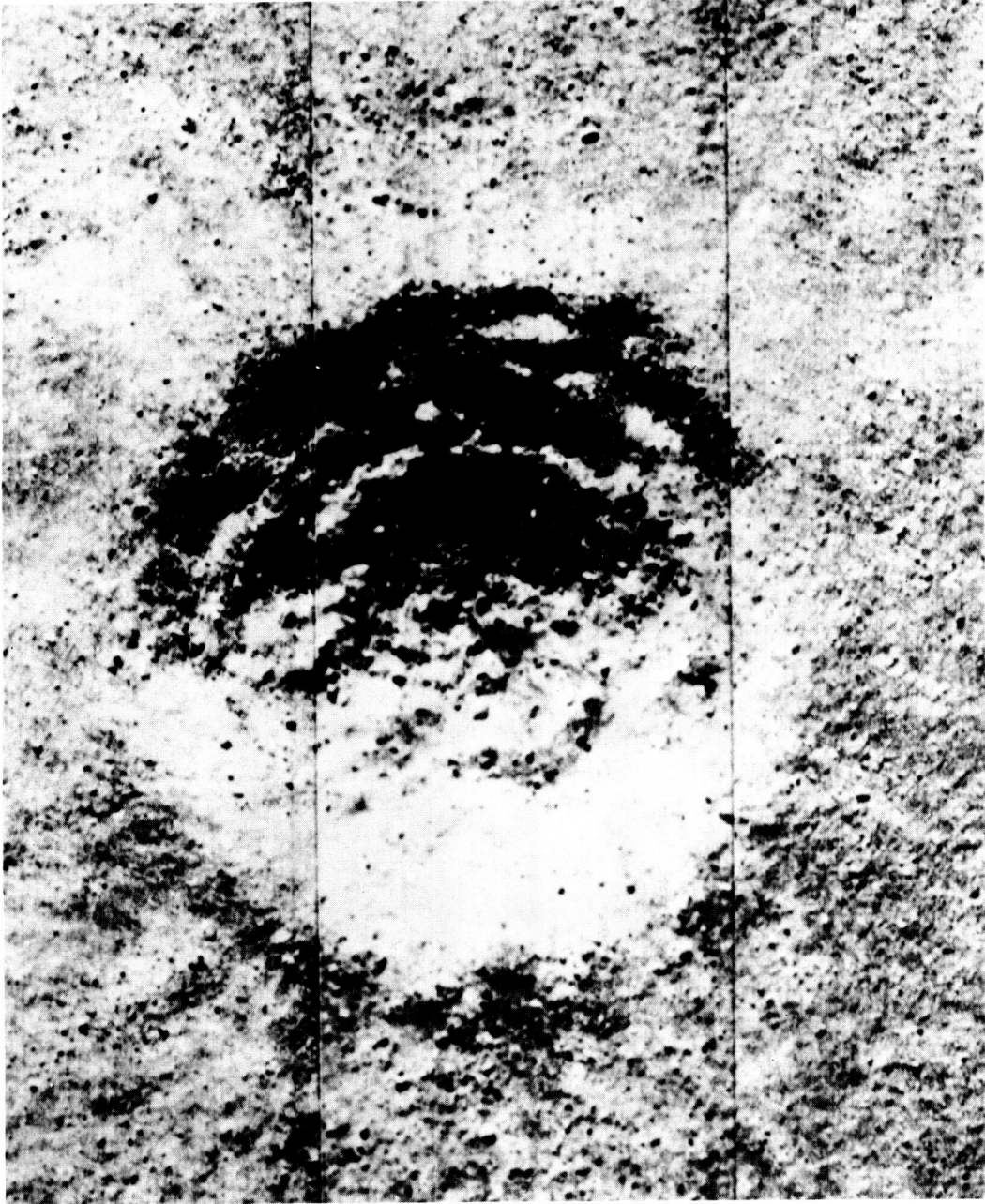


Figure 8a. Typical Large Fresh Lunar Crater (Orbiter II Site P-11B, Frame 177)
Diameter Approximately 385 Meters



Figure 8b. Danny Boy Crater at Buck Board Mesa, Nevada Test Site
Diameter Approximately 80 Meters (Moore)

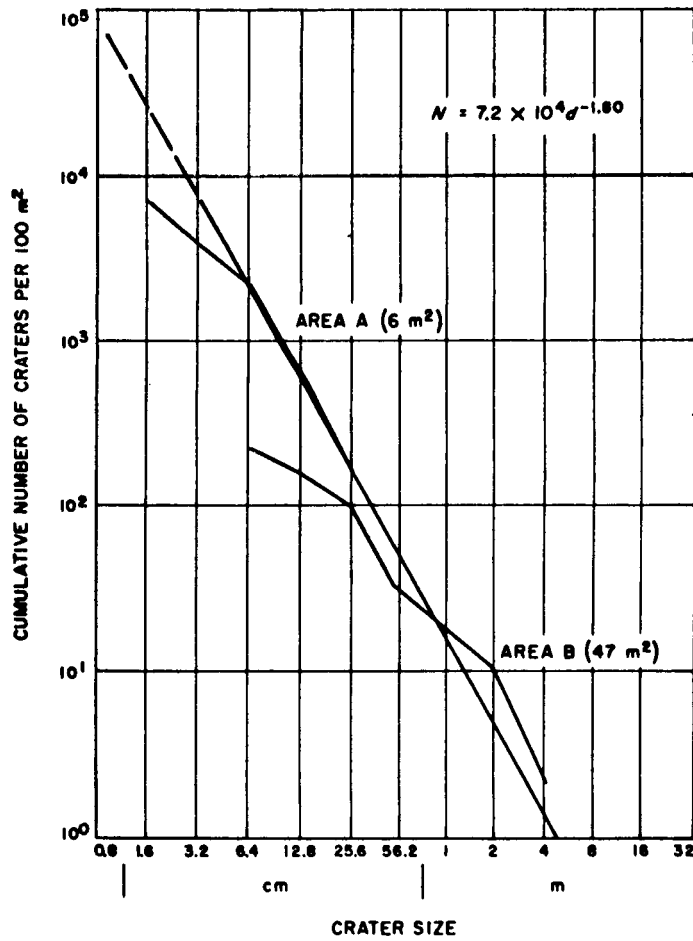


Figure 9a. Cumulative Size-Frequency distribution of Craters on Lunar Surface Determined from Surveyor I Pictures (Shoemaker)

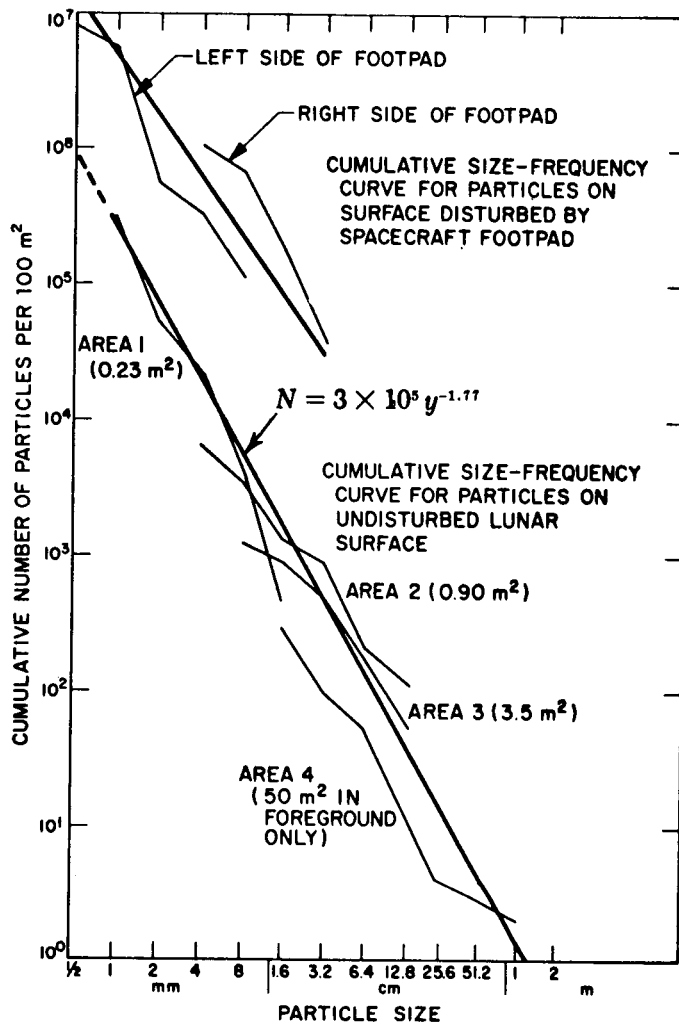


Figure 9b. Cumulative Frequency Distribution of Particles on Lunar Surface, as Determined from Surveyor I Pictures (Shoemaker)

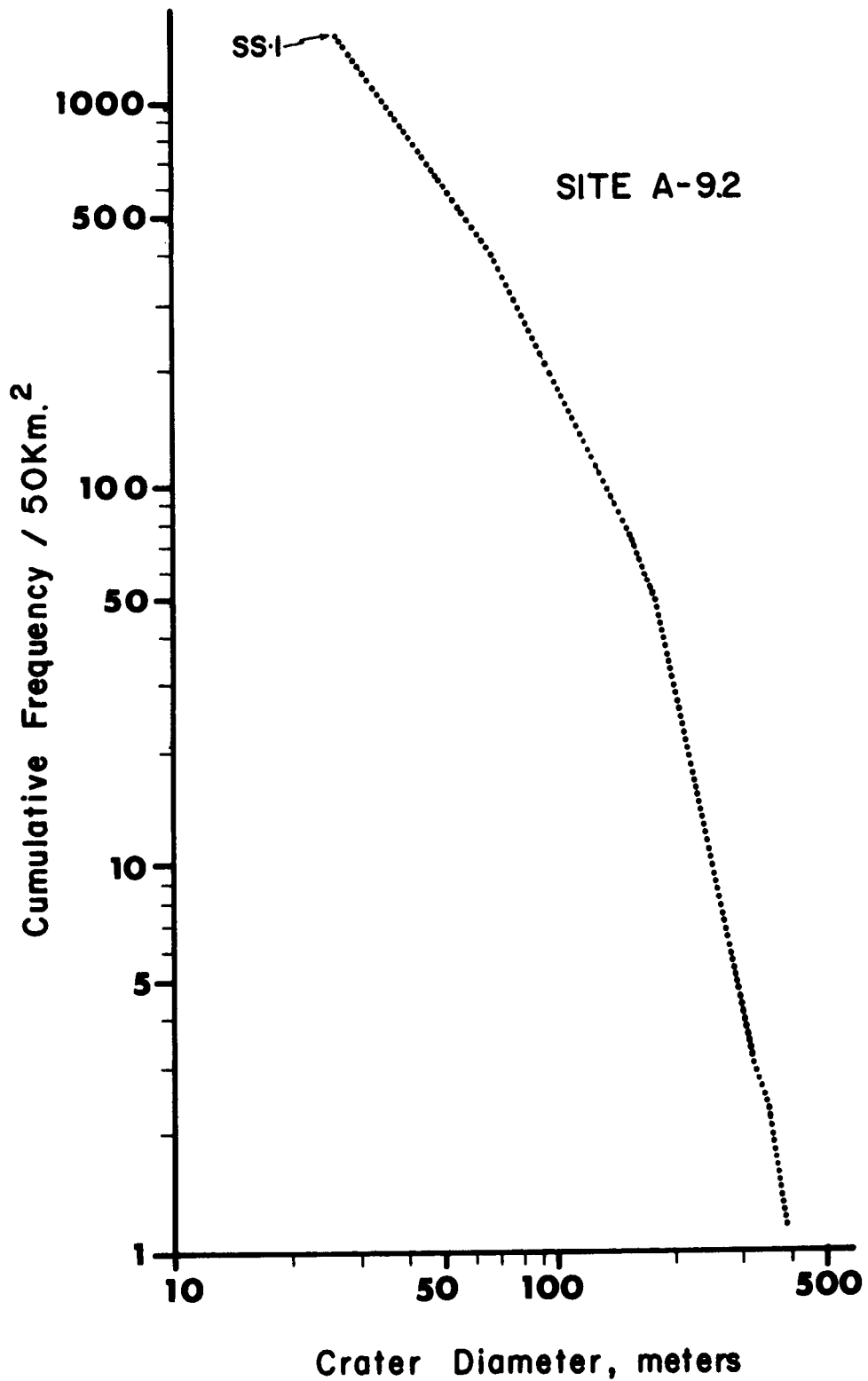


Figure 10. Cumulative Size Frequency Distribution of Craters on Lunar Surface at Surveyor I Area (A. Kelly & R. Lugin, USGS)

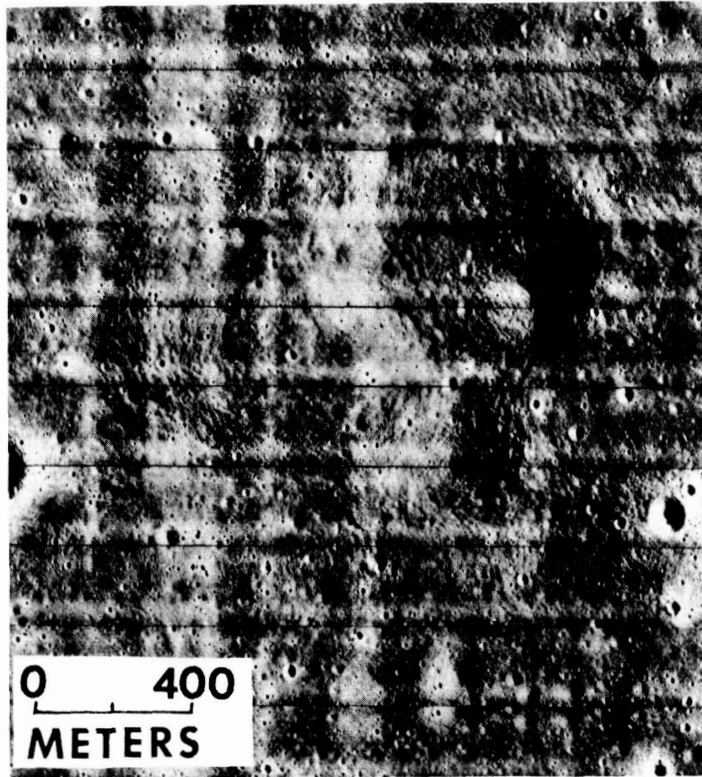


Figure 11. Slumping of Lunar Soil Toward Floor of Craters (Patterned Ground) (II-P-1 Frame H 13)

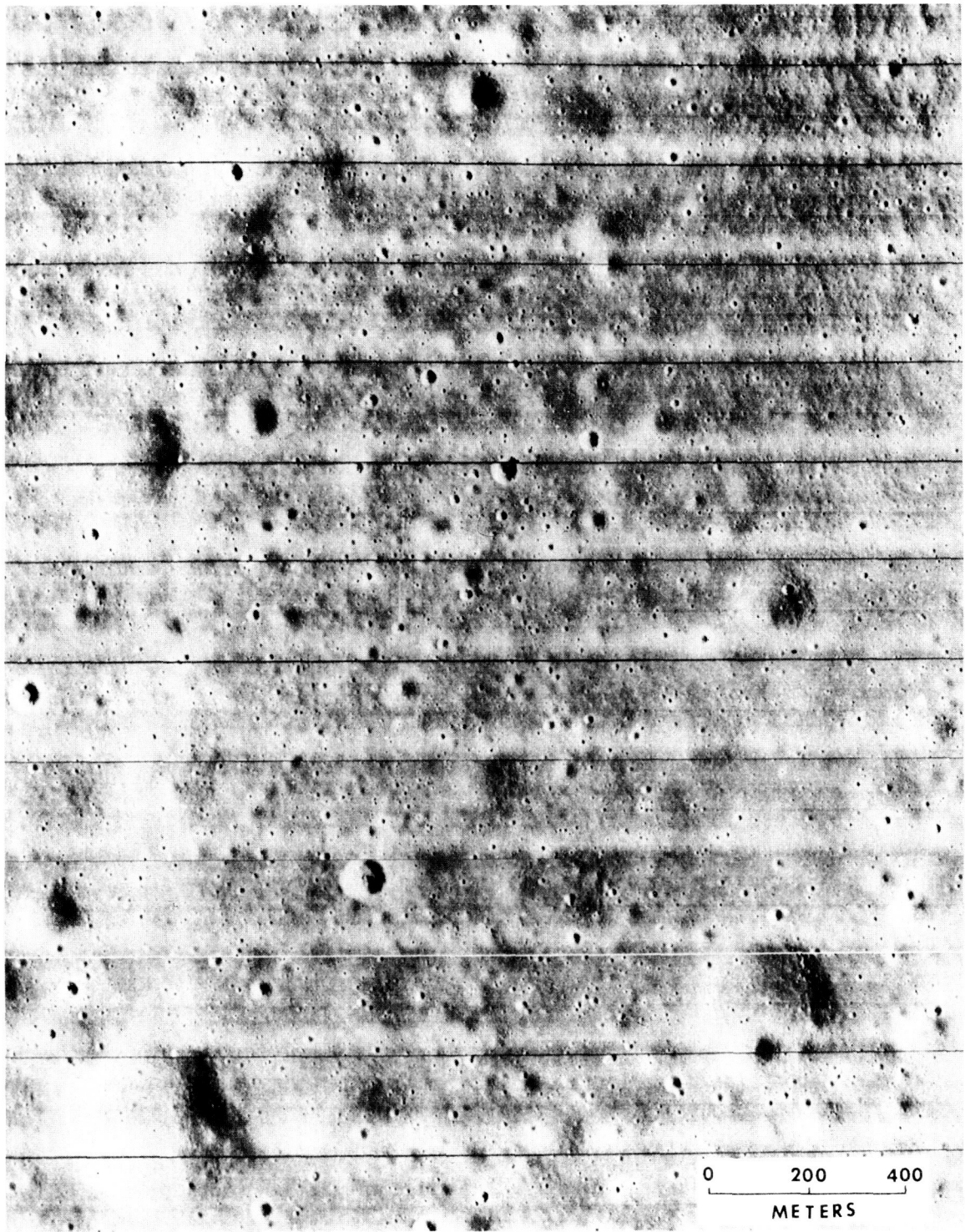
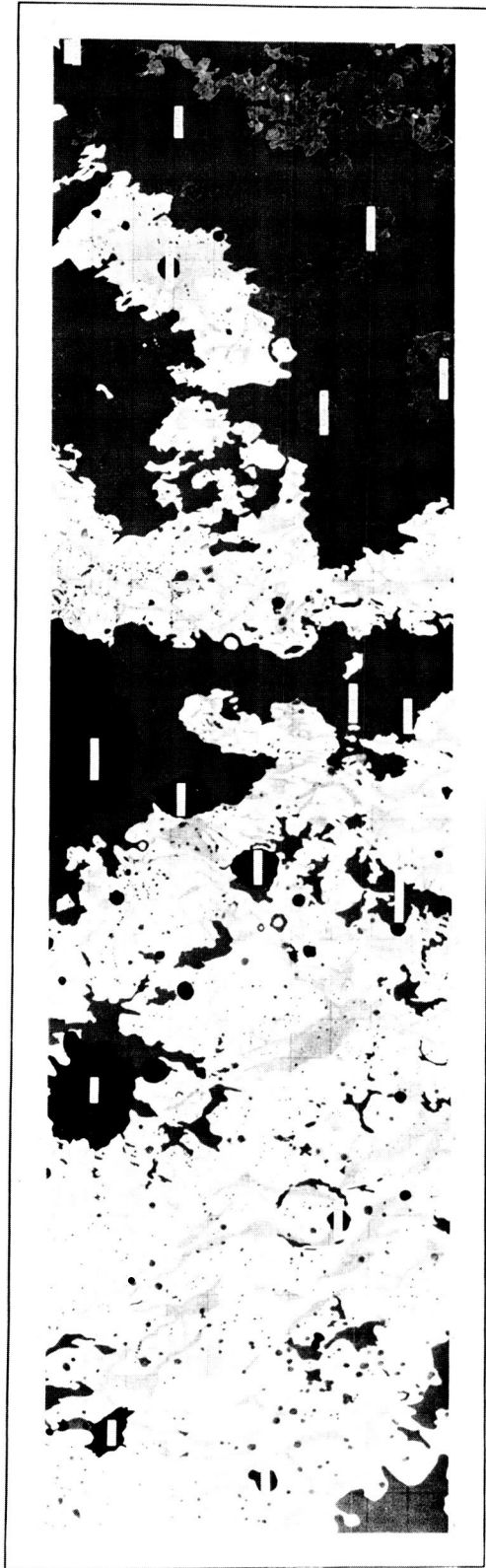


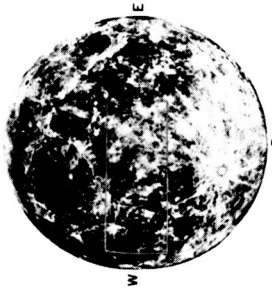
Figure 12. Possible Smooth Area due to Presence of Volcanic Materials (Orbiter II-P-11A, Frame H-165)



TERRAIN CLASSIFICATION OF THE LUNAR EQUATORIAL BELT (10 N-10 S, 60 W-15 E)
(PRELIMINARY EDITION, JULY 1964)

BY JOHN F. MCCAULEY

LOCATION OF MAP AREA



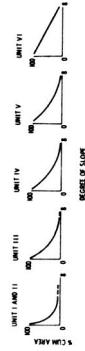
PREPARED BY THE U.S. GEOLOGICAL SURVEY
 NATIONAL AERONAUTICS AND SPACE ADMINISTRATION

EXPLANATION

- TOPOGRAPHIC CHARACTERISTICS:**
- UNIT I: SLOPE FREQUENCY RANGES FROM 10% TO 15%. GENERALLY CONSISTS OF THE HIGHEST PARTS OF THE MOUNTAINS.
 - UNIT II: SLOPE FREQUENCY RANGES FROM 15% TO 20%. GENERALLY CONSISTS OF THE HIGHEST PARTS OF THE MOUNTAINS AND LOWER SLOPE AREAS.
 - UNIT III: SLOPE FREQUENCY RANGES FROM 20% TO 25%. CONSISTS OF HILLS AND THE LOWER PARTS OF THE MOUNTAINS.
 - UNIT IV: SLOPE FREQUENCY RANGES FROM 25% TO 30%. CONSISTS OF HILLS AND THE LOWER PARTS OF THE MOUNTAINS.
 - UNIT V: SLOPE FREQUENCY RANGES FROM 30% TO 35%. CONSISTS OF HILLS AND THE LOWER PARTS OF THE MOUNTAINS.
 - UNIT VI: SLOPE FREQUENCY RANGES FROM 35% TO 40%. CONSISTS OF HILLS AND THE LOWER PARTS OF THE MOUNTAINS.
 - UNIT VII: SLOPE FREQUENCY RANGES FROM 40% TO 45%. CONSISTS OF HILLS AND THE LOWER PARTS OF THE MOUNTAINS.
 - UNIT VIII: SLOPE FREQUENCY RANGES FROM 45% TO 50%. CONSISTS OF HILLS AND THE LOWER PARTS OF THE MOUNTAINS.
 - UNIT IX: SLOPE FREQUENCY RANGES FROM 50% TO 55%. CONSISTS OF HILLS AND THE LOWER PARTS OF THE MOUNTAINS.
 - UNIT X: SLOPE FREQUENCY RANGES FROM 55% TO 60%. CONSISTS OF HILLS AND THE LOWER PARTS OF THE MOUNTAINS.
 - UNIT XI: SLOPE FREQUENCY RANGES FROM 60% TO 65%. CONSISTS OF HILLS AND THE LOWER PARTS OF THE MOUNTAINS.
 - UNIT XII: SLOPE FREQUENCY RANGES FROM 65% TO 70%. CONSISTS OF HILLS AND THE LOWER PARTS OF THE MOUNTAINS.
 - UNIT XIII: SLOPE FREQUENCY RANGES FROM 70% TO 75%. CONSISTS OF HILLS AND THE LOWER PARTS OF THE MOUNTAINS.
 - UNIT XIV: SLOPE FREQUENCY RANGES FROM 75% TO 80%. CONSISTS OF HILLS AND THE LOWER PARTS OF THE MOUNTAINS.
 - UNIT XV: SLOPE FREQUENCY RANGES FROM 80% TO 85%. CONSISTS OF HILLS AND THE LOWER PARTS OF THE MOUNTAINS.
 - UNIT XVI: SLOPE FREQUENCY RANGES FROM 85% TO 90%. CONSISTS OF HILLS AND THE LOWER PARTS OF THE MOUNTAINS.
 - UNIT XVII: SLOPE FREQUENCY RANGES FROM 90% TO 95%. CONSISTS OF HILLS AND THE LOWER PARTS OF THE MOUNTAINS.
 - UNIT XVIII: SLOPE FREQUENCY RANGES FROM 95% TO 100%. CONSISTS OF HILLS AND THE LOWER PARTS OF THE MOUNTAINS.

GENERAL INFORMATION

1:1,000,000



MS-O 64-54 DEC. 11, 1964

Figure 13a. Terrain Classification of Lunar Equatorial Belt

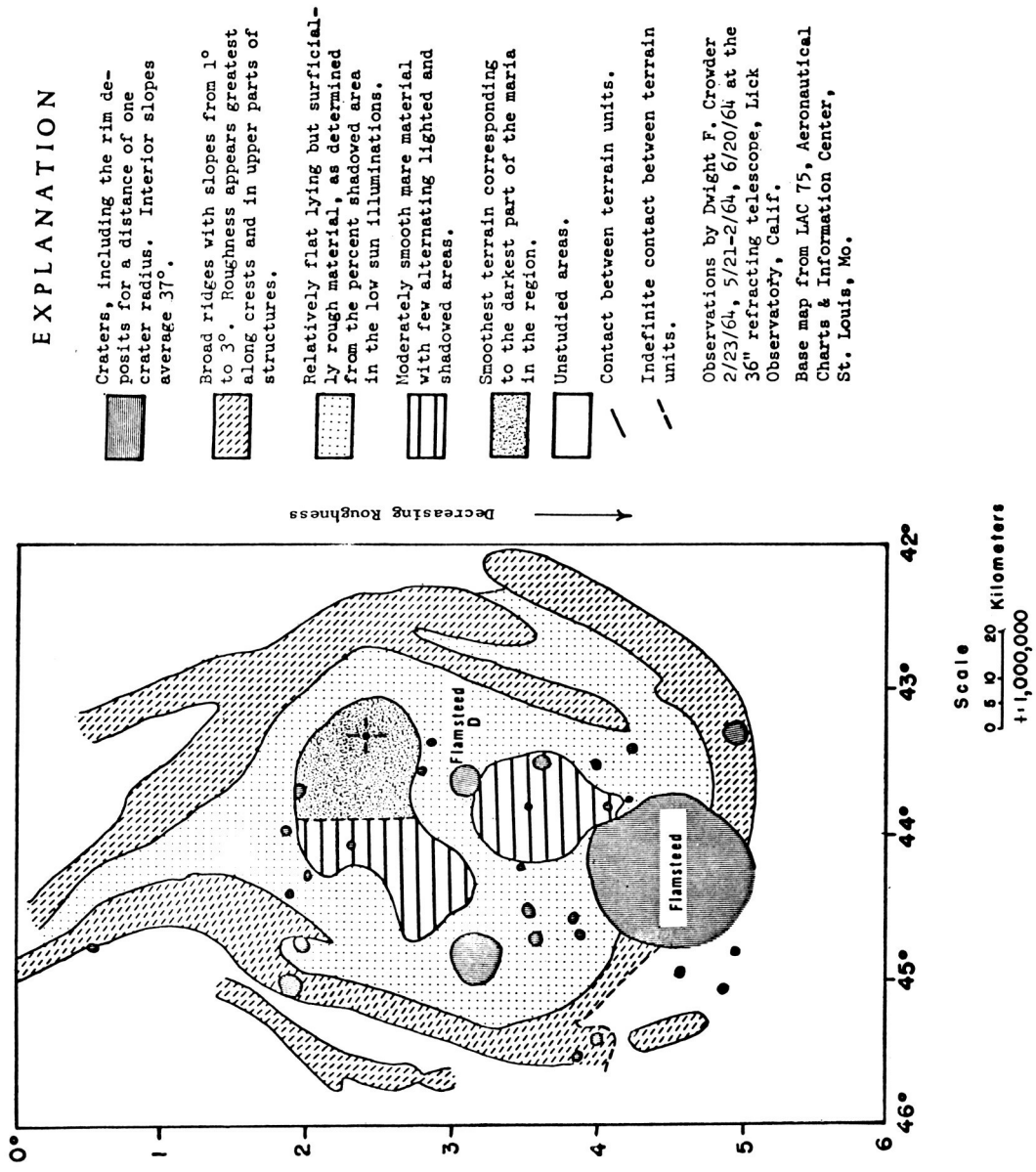


Figure 13b. Flamsteed Crater Terrain Analysis

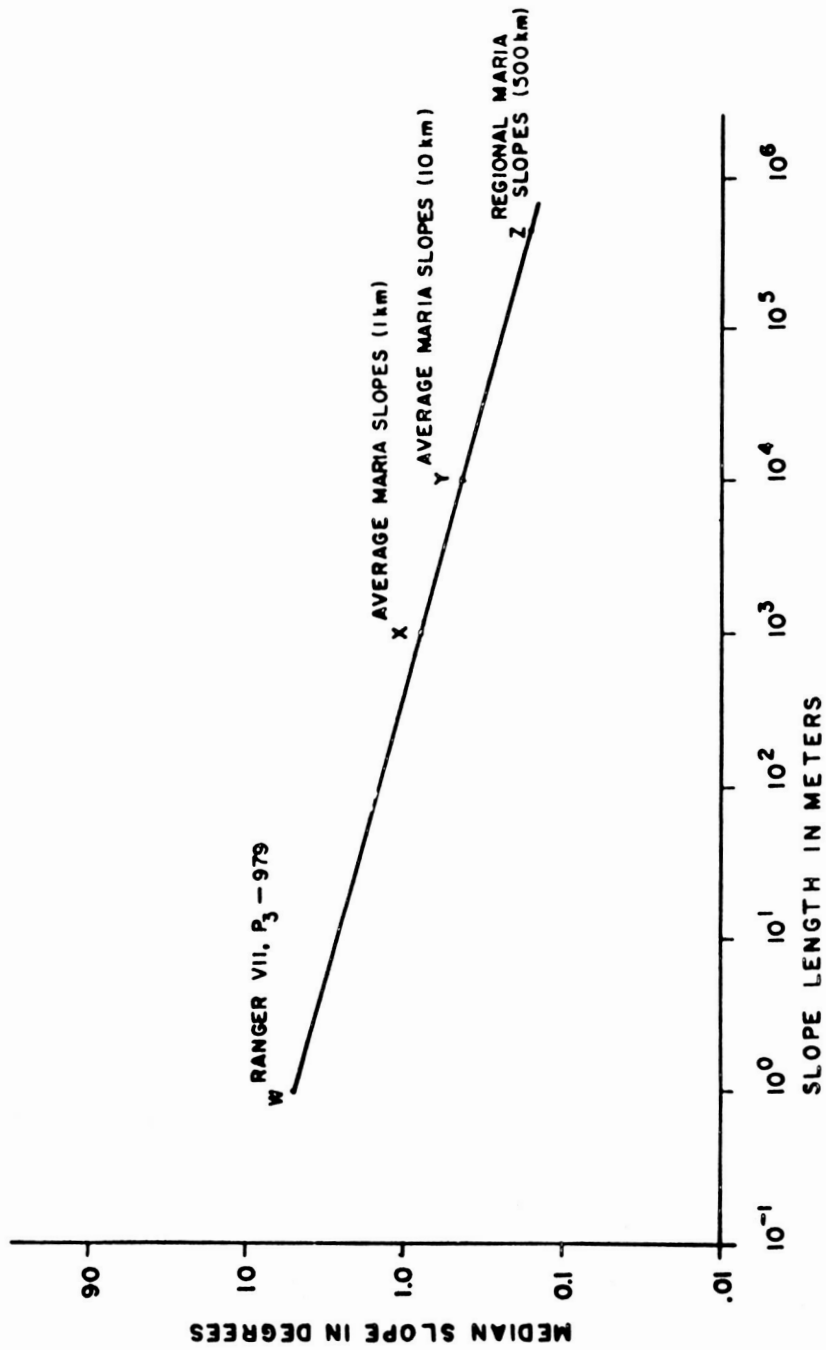


Figure 14. Median Slope Values Plotted as a Function of Slope Length (ΔL) for the Average Lunar Mare (after McCauley, 1964)

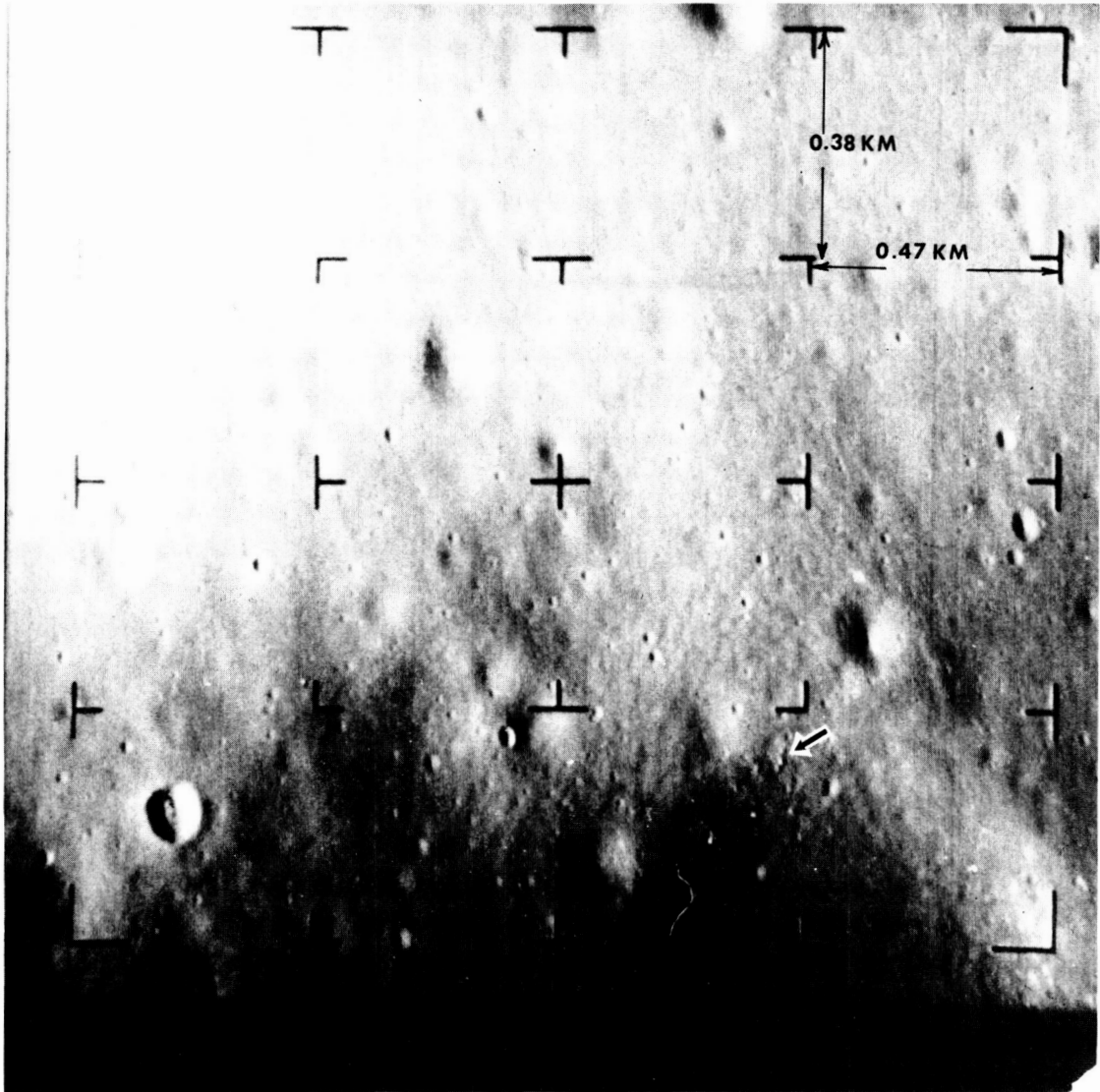


Figure 15. Blocky Material on Crater Rim Photographed by
Ranger 8, Frame No. 541

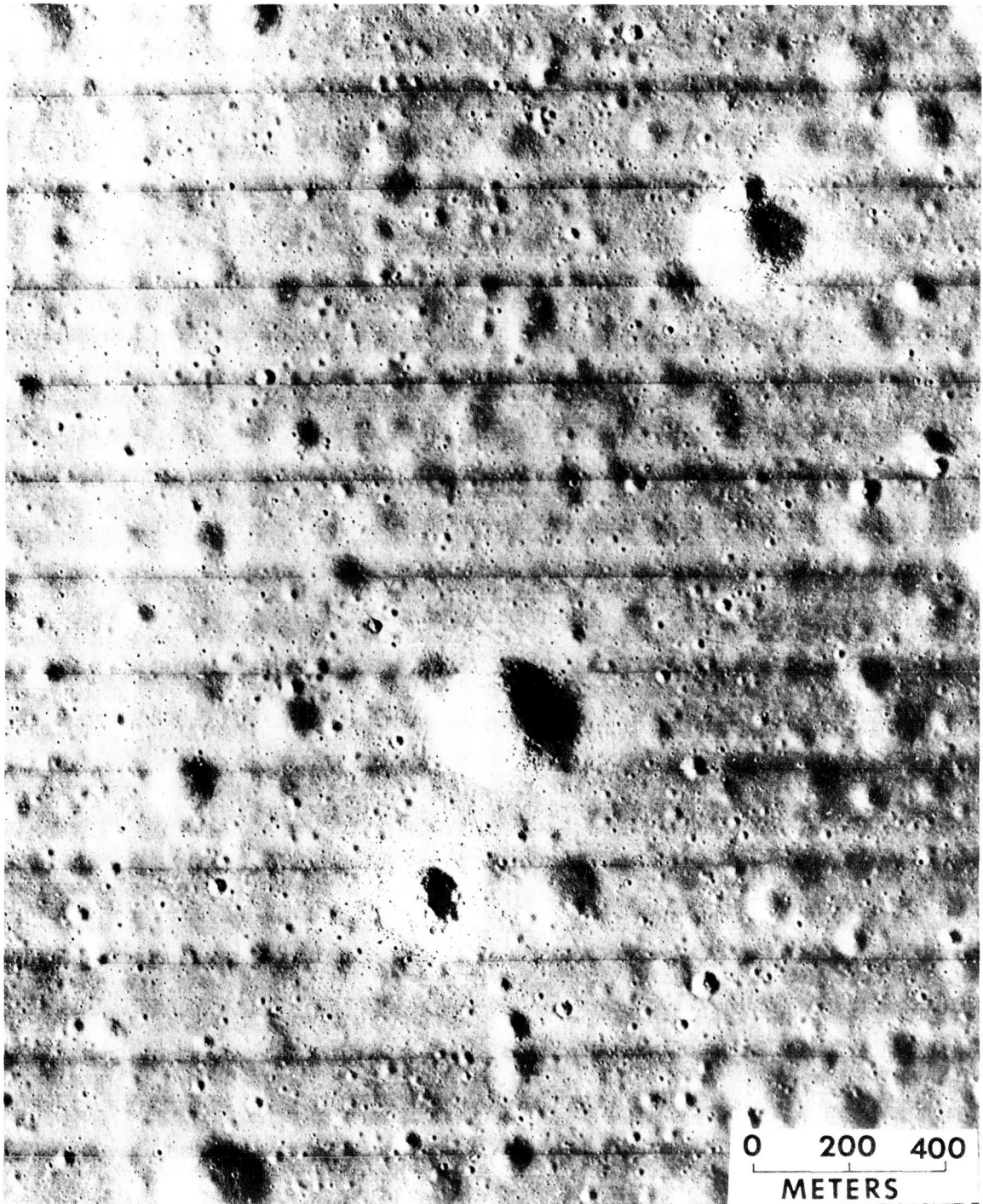


Figure 16. Typical Dark Regional Mare Terrain
(Orbiter III-P-12A, Frame 192)

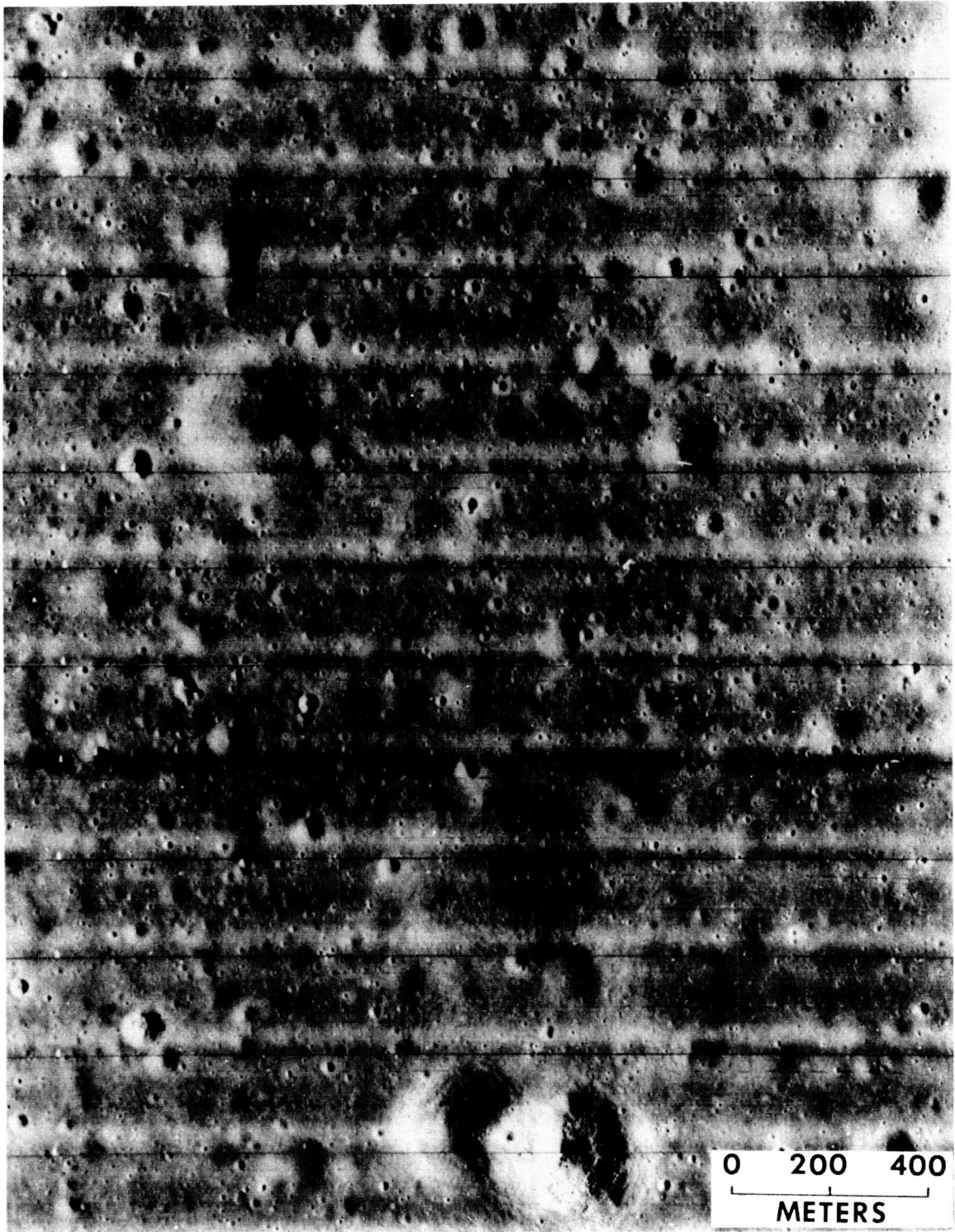


Figure 17. Typical Regional Mare Terrain (Orbiter II-P-8b, Frame H-128)

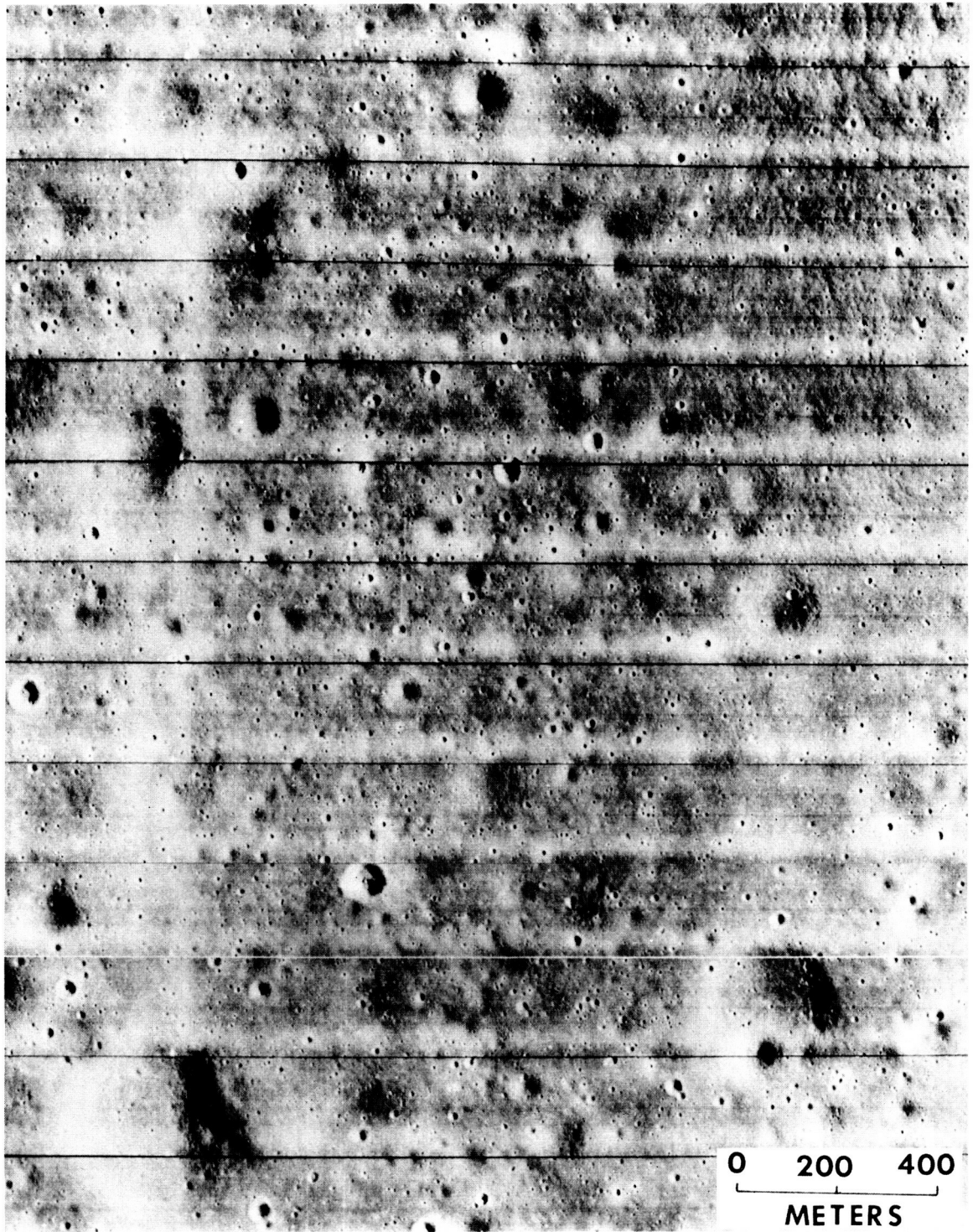


Figure 18. Typical Smooth-Rayed Mare Terrain
(Orbiter II-P-11A, Frame H-165)

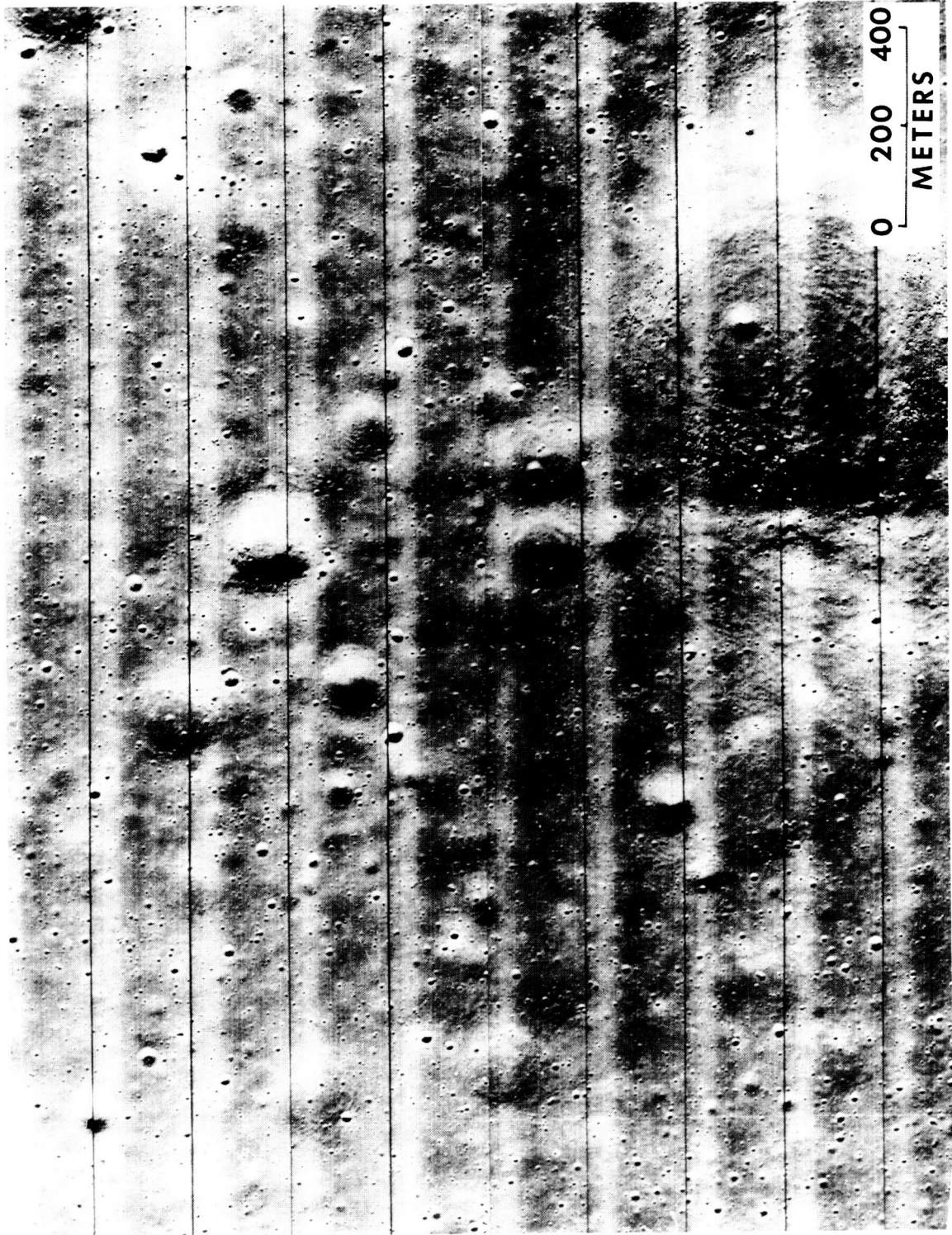


Figure 19. Typical Rough-Rayed Mare Terrain (Orbiter II-P-5, Frame H-70)

REFERENCES

1. Scott, R., "Lunar Scientific Model," JPL Project Document No. 54, December 15, 1966.
2. Lunar Surface: An Interpretation Based on Photographic Data from the Russian Luna IX and the United States Surveyor I, Aero-Astrodynamics Research Review No. 5, NASA TM X-53568, October 15, 1966.
3. Gault, D. E., W. L. Quaide and V. R. Oberbeck, "Interpreting Ranger Photographs from Impact Cratering Studies," Proc. Conference on the Nature of the Lunar Surface, GSFC, NASA-IAA meeting, Greenbelt, Md., April 1965.
4. Moore, H. J., "Ranger VIII and IX, Part II: Experimenters Analysis and Interpretations," JPL TR 32-800, March 15, 1966.
5. Lipskiy, Yu. N., A. I. Lebedinskiy, "Excerpts from TASS Communiques Luna 13 is on the Moon," Translation ST-PR-LPS-10-545, NASA-Goddard Space Flight Center, January 4, 1967.
6. Surveyor I Mission Report, Part III, Television Data, JPL Technical Report 32-1023, November 1, 1966.
7. Surveyor I, Mission Report, Part II, Scientific Data and Results, JPL Technical Report 32-1023, 1966.
8. McCauley, John F., "A Preliminary Report on the Terrain Analysis of the Lunar Equatorial Belt," U.S.G.S. Report, 1 July 1964.
9. Rowan, L. C. and John F. McCauley, "Lunar Orbiter-Image Analysis Studies Report," Progress Report, January 31, 1966, USGS/NASA Contract W-12, Manned Spacecraft Center.
10. Jaeger, R. M. and D. J. Schuring, "Spectrum Analysis of Terrain in Mare Cognitum," J.G.R., Vol. 71, No. 8, April 1966.
11. Van Deusen, B. D., "A Statistical Technique for the Dynamic Analysis of Vehicles Traversing Rough Yielding and Non-Yielding Surfaces," NASw-1287, Chrysler Corp., May 1966.
12. R. Choate, "Lunar Scientific Model," JPL Project Document No. 54, December 15, 1966.
13. Fields, S. A. et al., "Surface Mining on the Moon," Paper presented at Fifth Annual Meeting of the Working Group on Extraterrestrial Resources, March 1-3, 1967, Huntsville, Ala.
14. Smith, B. C., Journal Geophysical Research, Vol. 72, No. 4, Feb. 15, 1967, pp. 1398-1399.

SUPPORTING DOCUMENTS

1. Rowen, L. C., "The Physics of the Moon," Publications of the American Astronautical Society, Orbiter Observations of the Lunar Surface, 29 December 1966.
2. Lunar Environment Analysis, TR-293-6-002E, "A Survey of Lunar Surface Models," NAS8-20082 Northrop Space Laboratories, Huntsville, Alabama, 11 November 1966.
3. Lunar Scientific Model, JPL Project Document No. 54, December 1966.
4. The Lunar Surface: Interpretations of Data from Ranger VII, VIII, IX, and the Surveyor Mission, R-AERO-Y-123-66, September 30, 1966.
5. Preliminary Terrain Evaluation and Apollo Landing Site Analysis Based on Lunar Orbiter I Photography, Report LWP-326.
6. Preliminary Geologic Evaluation and Apollo Landing Site Analysis Based on Orbiter II Photography Report, Report LWP-363.

LUNAR ENVIRONMENT: DESIGN CRITERIA MODELS FOR USE
IN LUNAR SURFACE MOBILITY STUDIES

By


Otha H. Vaughan, Jr.

The information in this report has been reviewed for security classification. Review of any information concerning Department of Defense or Atomic Energy Commission programs has been made by the MSFC Security Classification Officer. This report, in its entirety, has been determined to be unclassified.

This document has also been reviewed and approved for technical accuracy.



W. W. Vaughan
Chief, Aerospace Environment Division



E. D. Geissler
Director, Aero-Astroynamics Laboratory

DISTRIBUTION

DIR

R-DIR

Mr. Weidner

DEP-T

Dr. Rees

R-ASO

Mr. Williams (2)
Mr. Carter
Mr. Huber
Mr. Hamby
Mr. Spears
Mr. Woodcock
Mr. Bradford
Mr. Brown
Mr. Madewell
Mr. Schaefer
Mr. Tidd

R-ASTR

Dr. Haeussermann
Mr. Digesu (2)
Mr. Hamilton
Mr. Hosenthine
Mr. Dodds
Mr. Moore
Mr. Wagnon
Mr. Brandner

R-EO

Dr. Johnson

R-ME

Mr. Kuers
Mr. Maus
Mr. Groth

R-P&VE

Dr. Lucas
Mr. Hellebrand
Mr. Goerner (2)
Mr. Johns (3)
Mr. Darwin
Mr. Laue
Mr. deSanctis
Mr. Vaccaro
Mr. Paul

R-QUAL

Mr. Grau

R-SS

Dr. Stuhlinger (2)
Mr. Downey (5)
Mr. Bensko
Mr. Wells
Dr. Hale
Dr. Shelton
Mr. Dozier
Mr. Heller

I-DIR

Brig. Gen. O'Connor

I-SAA

Mr. Belew
Mr. Reinartz
Mr. Stewart

I-MO-MGR

Dr. Speer (2)

RSIC

MS-IP

MS-IL (8)

MS-H

I-RM-M

CC-P

MS-T (5)

R-AERO

Dr. Geissler
Mr. Jean
Mr. Dahm
Mr. Horn
Mr. Lindberg
Mr. Baker
Mr. McNair
Mr. Thomae (5)
Mr. Cummings
Dr. Heybey
Mr. Lavender
Mr. Murphree
Dr. H. Krause
Mr. Dalton
Mr. Daniels

DISTRIBUTION (Continued)

R-AERO (cont'd)

Mr. Fichtl
Mr. Kaufman
Mr. O. Smith
Mr. R. Smith
Mr. O. Vaughan (40)
Mr. W. Vaughan (2)

EXTERNAL DISTRIBUTION

Office of Manned Space Flight
NASA Headquarters
Washington, D. C., 20546
Attn: Dr. George Mueller, Director
Mr. P. Grosz (3)
Mr. N. Peil
Mr. W. Green

Office of Advanced Research and Technology
NASA Headquarters
Washington, D. C., 20546
Attn: Mr. M. Charak (2)
Mr. M. Ames
Mr. W. Keller

Office of Space Science and Applications
NASA Headquarters
Washington, D. C., 20546
Attn: Dr. W. B. Foster (2)
Dr. J. Naugle
Mr. E. Cortright
Dr. Fellows
Dr. Dubin
Dr. Gerathewohl

NASA - Ames Research Center
Moffett Field
Mountain View, Calif., 94035
Attn: Dr. S. J. DeFrance, Director
Library

Scientific and Technical Information Facility (25)
Box 33
College Park, Md.
Attn: NASA Representative (S-AK/RKT)

EXTERNAL DISTRIBUTION (Continued)

NASA-Manned Spacecraft Center
Houston, Texas, 77001
Attn: Dr. R. R. Gilruth, Director
Mr. Christopher Craft
Mr. Donald K. Slayton
Dr. Hess (2)
Dr. J. Dietrich
Technical Library (2)

Air Force Cambridge Research Laboratories
Bedford, Mass.
Attn: CRFL, Dr. J. W. Salisbury (2)
Technical Library

Bellcomm, Inc.
1100 17th St. N. W.
Washington, D. C.
Attn: Mr. D. R. Valley

Kennedy Space Flight Center
Cocoa Beach, Fla. 32931
Attn: Technical Library

Langley Research Center
Langley Field, Va.
Attn: Dr. F. L. Thompson, Director
Library

Goddard Space Flight Center
Greenbelt, Md., 20771
Attn: Dr. J. Clark, Director
Mr. D. C. Kennard, Jr.
Dr. J. O'Keefe
Dr. P. Lowman
Library

Jet Propulsion Laboratory
California Inst. of Tech.
4800 Oak Grove Dr.
Pasadena 3, Calif., 91103
Attn: Dr. Conway Sydner
Mr. R. Choate
Dr. L. Jaffee
Dr. A. Loomis
Library

EXTERNAL DISTRIBUTION (Continued)

Lewis Research Center
21000 Brookpark Rd.
Cleveland, Ohio, 44135
Attn: Dr. Abe Silverstein, Director
Library

U. S. Geological Survey
Branch of Astrogeological Studies
345 Middle Field Rd.
Menlo Park, Calif. 94025
Attn: Dr. H. Masursky (5)
Dr. D. Wilhelms
Dr. H. Moore

U. S. Geologic Survey
Center of Astrogeology
601 East Cedar Ave.
Flagstaff, Arizona, 8600
Attn: Dr. L. Rowan (5)
Dr. J. Ulrich (5)
Dr. H. Pohn
Dr. J. McCauley
Dr. E. Shoemaker

Dr. James A. Van Allen
State University of Iowa
Iowa City, Iowa

Commander (2)
Headquarters, Air Weather Service
Scott Air Force Base, Illinois

Air Force Systems Command (2)
Space Systems Division
Air Force Unit Post Office
Los Angeles 45, California

Meteorological & Geostrophysical Abstracts
P. O. Box 1736
Washington 13, D. C.